The Crystal Structure of Iron Particles Dispersed in a Glasslike Carbon Matrix

Mamoru OMORI,* Toshio HIRAI,* and Seishi YAJIMA

The Oarai Branch, The Research Institute for Iron, Steel and Other Metals, Tohoku University, Oarai, Ibaraki 311-13

(Received October 24, 1977)

Ultra-fine iron particles were dispersed in a glasslike carbon matrix by the heat treatment of acetylferrocene-furfural resins. The dispersed iron particles were investigated by means of X-ray and electron diffraction analyses and by means of electron microscopy. In resins heat-treated at 400 °C, iron particles of varying diameters were observed by means of electron microscopy. The crystal structure of the iron particles was analyzed by means of X-ray and electron diffractions. Finely subdivided iron particles were identified as hexagonal, close-packed (hcp) and expanded, body-centered cubic (bcc) irons. The hcp iron is the high-pressure phase of iron metal. The ultra-fine iron particles were coagulated to larger particles by heat treatment above 400 °C. The size of their unit cell was the same as that of standard bcc iron.

Considerable interest is being devoted to the study of ultra-fine particles of metals and metal compounds because many of their properties are essentially different from those in the bulk state. Fine particles are prepared by means of the evaporation and condensation of metal in an inert gas at a low pressure. In the fine particles of chromium (>100 Å), a new class of crystals has been observed.[1,2] As the particle size of ferromagnetic material is reduced to a diameter of 10—100 Å, it shows a ferromagnetic-to-superparamagnetic transition. By the use of ferromagnets dispersed in glass and zeorite matrices, their superparamagnetic behavior has been investigated.[3-7] Ultra-fine particles of iron and cobalt, less than about 30 Å in diameter, which have been prepared by electrodeposition onto mercury, are superparamagnetic.[8,9] Superparamagnetic cobalt particles (<14 Å) are prepared by precipitation into Cu–2%Co alloy.[10,11] Ultra-fine nickel particles (<50 Å) are reduced from $Ni(NO_3)_2$ in a silica gel and are superparamagnetic.[12,13] Ferrite particles whose diameters are less than about 100 Å have superparamagnetic properties.[14,15] Moreover, atomic metals have been prepared in the matrices of inert gas from the vapour of metals at the temperature of liquid helium.[16-18]

As has been reported in previous papers, ultra-fine iron particles have been prepared in a glasslike carbon matrix by the heat treatment of acetylferrocene–furfural resins.[19-21] Their particle size varies with the iron content in the resin. The dispersion of iron particles is markedly related to the resin structure. The ultra-fine particles are not prepared by the heat treatment of ferrocene–phenol resin, which is different in structure from the acetylferrocene–furfural resin.[22] The glasslike carbon is stable at elevated temperatures, and does not show any strong peaks in X-ray and electron diffractions. Its absorption coefficient for X-rays and an electron beam is small, since it is an amorphous compound consisting of carbon, hydrogen, and oxygen. Therefore, the iron particles dispersed in the glasslike carbon matrix are favorable for the X-ray and electron diffraction analyses and for electron-microscopic observations.

In the present investigation, the crystal structure and size of iron particles dispersed in the glasslike carbon matrix were studied in detail. The iron atoms were liberated from ferrocene skeletons in the acetylferrocene-furfural resin by heat treatment at 400 °C. The liberated iron coagulated to ultra-fine iron particles of various sizes. The ultra-fine iron particles were coagulated in the glasslike carbon matrix by the irradiation of the electron beam and by heat treatment above 400 °C. The crystal structure of these iron particles was then analyzed by means of X-ray and electron diffractions. The size and shape of the particles were observed by means of an electron microscope.

Experimental

Preparation and Pyrolysis of Resins. The synthesis of acetylferrocene–furfural resin was described in a previous paper.[23] When the molar ratio of furfural (F) to acetylferrocene (A) in the starting material exceeded the F/A ratio of 15, the resin was not obtained. Acetone was added to the starting material containing furfural a more than the F/A ratio of 15. The furfural (1 mol) was mixed with 0.2 mol of acetylferrocene and acetone. To the mixture, concentrated sulfuric acid was then added until it amounted to 4 wt% of the total weight of furfural, acetylferrocene, and acetone. The subsequent treatment to get the resin was done in the way reported previously.[23] The resin was heated in an electric furnace under a vacuum as follows: 100—350 °C, 3.5 h; 350—400 °C, 2 h; 400—1500 °C, 100 °C/h. The heating was stopped at the desired maximum temperature. The heat-treated resin was then cooled to room temperature in an electric furnace. The heat-treated resin in a vacuum container was placed in the glovebox replaced with argon gas. The following operating procedures were carried out in the glovebox. The heat-treated resin was ground to powder using an agate mortar and a pestle. For X-ray diffraction measurements, the fine powdered sample, which had been passed through a 325-mesh screen, was loaded into a thin glass capillary and then sealed with silicone grease. The powdered sample for electron-microscopic measurements was placed in a glass tube filled with anhydrous hexane and then sealed with a rubber cap.

Elemental Analysis and Measurement of Properties. The determination of the iron was carried out with a Hitachi-207 atomic absorption spectrophotometer. The apparent densities were calculated from the weight and size of the resins.

* Present address: The Research Institute for Iron, Steel and Other Metals, Tohoku University, Sendai 980.

Table 1. Polycondensation of acetylferrocene and furfural

	Molar concentration			Elemental analysis (wt %)			Density (g/cm^3)
	Acetylferrocene	Furfural	Acetone	Fe	C	H	
2-Resin	1	2	0	12.2	64.98	4.29	1.43
5-Resin	1	5	0	9.08	64.01	3.77	1.43
10-Resin	1	10	0	7.51	62.50	3.95	1.02
20-Resin	1	20	3	3.14	63.56	4.01	0.976
30-Resin	1	30	5	2.26	63.65	3.91	0.968
40-Resin	1	40	7	1.67	62.16	3.49	0.973
100-Resin	1	100	19	0.81	63.16	3.62	0.947
Furan resin	0	5	1	0	63.04	3.11	0.946

The X-ray diffraction patterns were recorded on a Rigaku Geigerflex diffractometer using a Debye-Scherrer camera, Fe $K\alpha$ radiation, and a Mo filter. Electron-microscopic observation was carried out by using a JEM-100B transmission electron microscope at a direct magnification of 150000.

Results and Discussion

The synthetic results for acetylferrocene–furfural resins are summarized in Table 1. The structure of acetylferrocene–furfural resin has already been elucidated.[23] Ferrocene skeletones form a main chain in the structure. It is evident that the resin is stable above 300 °C, since the IR spectrum of resin does not change up to 300 °C. Upon heating the resin at 400 °C, though, all the absorption bands in the IR spectrum disappear.[23] Therefore, the resin can be concluded to be destroyed and converted into a glasslike carbon containing iron. It seems likely that the iron atom in the ferrocene skeleton is liberated and then forms an iron metal or its compound. When ferrocene is pyrolyzed above 400 °C, the iron metal is liberated from it. The liberated iron does not react with carbon, since iron carbides are not detected in the pyrolyzed product.[24] Moreover, body-centered cubic (bcc) iron is the only product when a graphite–$FeCl_3$ intercalate compound is heated at 950 K for 3 h.[25] Therefore, iron carbides are not produced from the liberated iron in the heat-treated resin. In addition, the formation of iron oxides has to be taken into account, since the glasslike carbon contains oxygen. It is well known that an iron monoxide is reduced with carbon at 350 °C *in vacuo*.[26] Therefore, it was considered that the liberated iron did not react *in vacuo* with the oxygen contained in the glasslike carbon. In the heat-treated resins, 10-Resin heat-treated at 400 °C [10-Resin (400 °C)] was pyrophoric on exposure to air. However, the pyrophoric phenomenon was not observed in the resin heat-treated above 400 °C. As is shown in Table 2, the quantity of hydrogen and oxygen in heat-treated resins decreased with an increase in the heat-treatment temperature, in a manner analogous to that of heat-treated glasslike carbons.[27] The iron contents of heat-treated resins increased with an increase in the heat-treatment temperatures (400—1200 °C). However, the iron contents of resins (1500 °C) decreased compared with those of resins (1200 °C). The decrease in the iron content was due to the higher vapour pressure of iron metal than that of carbon at high temperatures.[28]

Electron-microscopic Observation. The transmission electron micrographs of resins (400 °C) are shown in Photo. 1: Micrographs (1-1 and 1-2) correspond to the bright-field image of 2-Resin (400 °C); 1-3, 1-4, 1-5, 1-6, and 1-7, to the bright-field images of 10-, 10-, 30-, 40-, and 100-Resins (400 °C) respectively. The transmission electron micrograph (1-8) is based on Furan resin (400 °C). In the micrograph (1-1), iron particles 10—25 Å in diameter were uniformly dispersed, while larger iron particles (30—150 Å) were only thinly scattered. These iron particles coagulated upon irradiation by a strong electron beam, as is shown in Photo. 1-2. The coagulation of iron particles was due to the heat generated by the irradiation of the electron beam. In the case of 5-Resin (400 °C), the uniform dispersion of iron particles (10—25 Å) was similar to that of 2-Resin (400 °C). This uniform dispersion can be observed in

Table 2. Elemental analysis of heat-treated resins (wt %)

Sample	Heat treatment (°C)											
	400			800			1200			1500		
	Fe	C	H	Fe	C	H	Fe	C	H	Fe	C	H
2-Resin	13.20	69.07	3.68	19.1	76.01	0.61	21.2	76.43	0.15	19.1	80.49	0.06
5-Resin	10.60	71.08	3.22	13.8	80.54	0.63	15.6	81.31	0.33	15.9	83.27	0.07
10-Resin	7.96	72.01	3.58	12.1	81.01	0.50	12.9	81.90	0.29	11.7	87.96	0.09
20-Resin	3.65	73.33	3.65	4.47	87.01	0.71	6.45	88.20	0.31	5.87	93.55	0.02
30-Resin	2.54	75.06	3.77	4.13	87.31	0.51	4.45	90.12	0.16	3.32	95.77	0.03
40-Resin	2.06	76.36	3.69	3.41	87.87	0.66	3.50	91.40	0.21	2.90	96.23	0.09
100-Resin	1.00	77.14	3.78	1.10	89.90	0.61	1.82	93.28	0.31	0.98	98.43	0.10

the micrograph (1-3) of 10-Resin (400 °C). However, iron particles of irregular sizes (10—150 Å) were dispersed in the other part of the 10-Resin (400 °C), as is shown in Photo. 1-4. Since the density of 10-Resin was less than that of 2- and 5-Resins, the coagulation of iron must be greatly affected by the small difference in the heating temperature in the resin. Iron particles of irregular sizes (10—100 Å) were also observed in the glasslike carbon matrix of 30-Resin (400 °C). However, the number of iron particles in it was less than in 10-Resin (400 °C). No iron particles were found in the glasslike carbon of 40-Resin (400 °C), as is shown in Photo. 1-6. This indicates that the iron particles are subdivided into finer particles less than about 10 Å in diameter and which cannot be detected by means of the electron microscope. In the case of 100-Resin (400 °C), the iron particles were similarly less than about 10 Å in diameter. The transmission electron micrographs of 40- and 100-Resins (400 °C) were the same as that of Furan resin (400 °C). The size of the iron particles, as observed by means of the electron microscope, is shown in Table 3. The iron

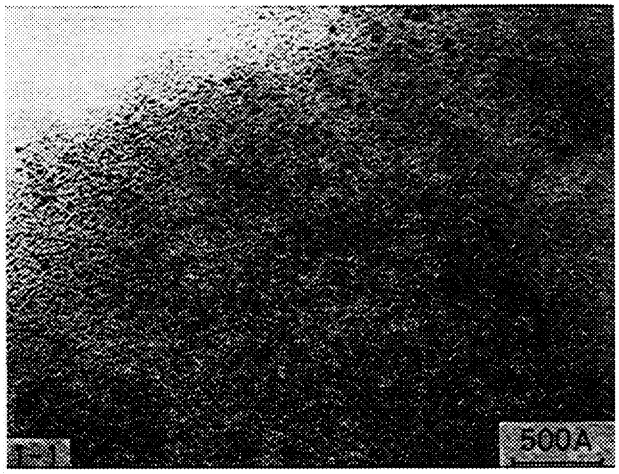

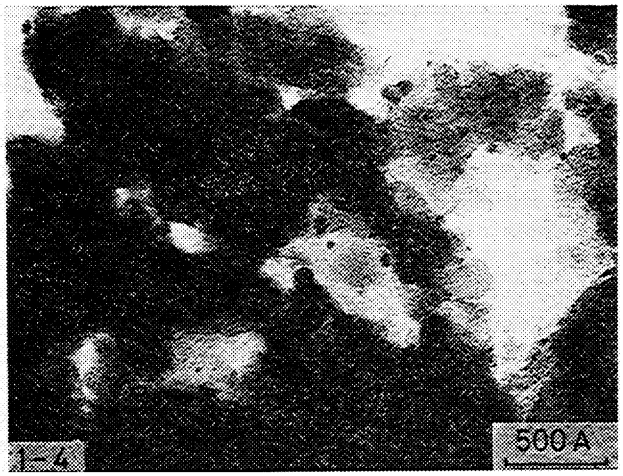

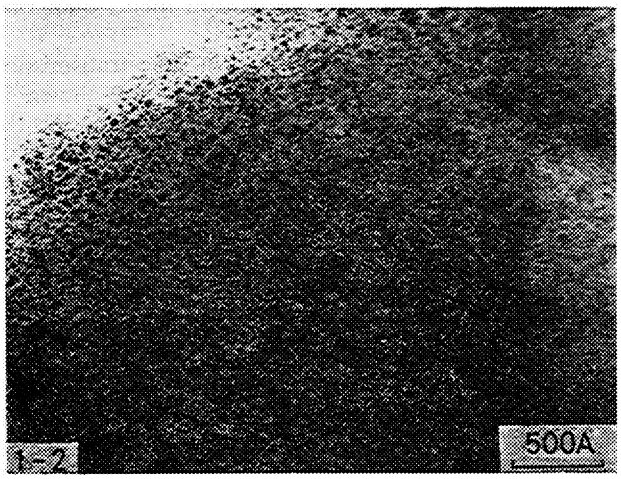

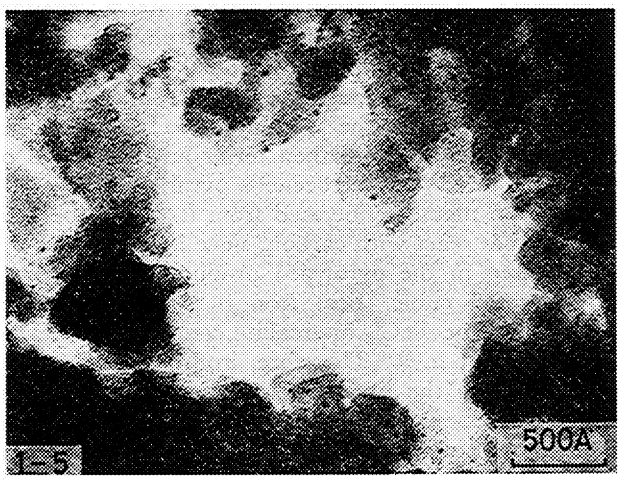

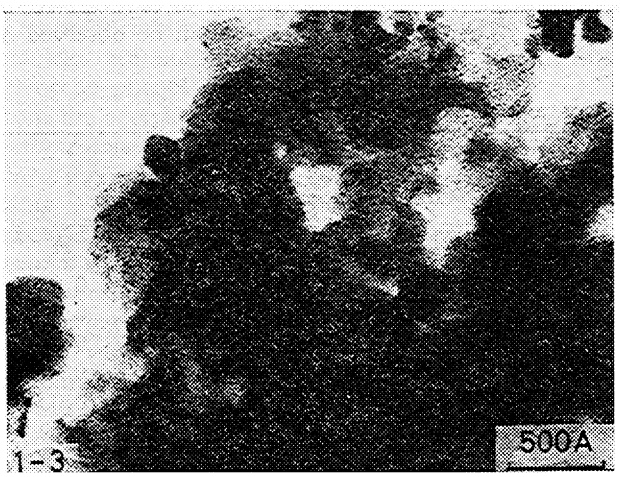

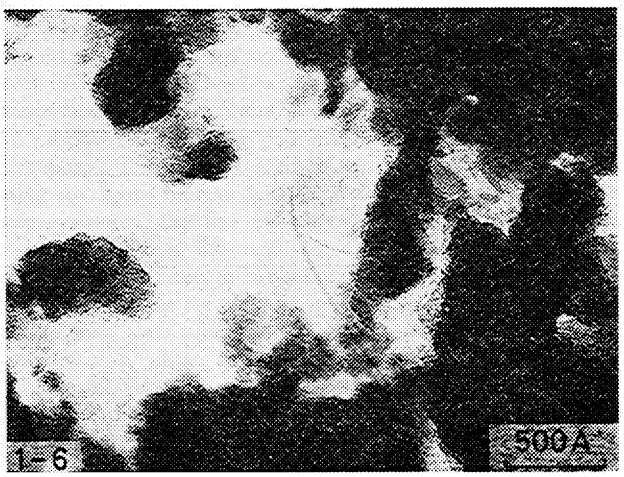

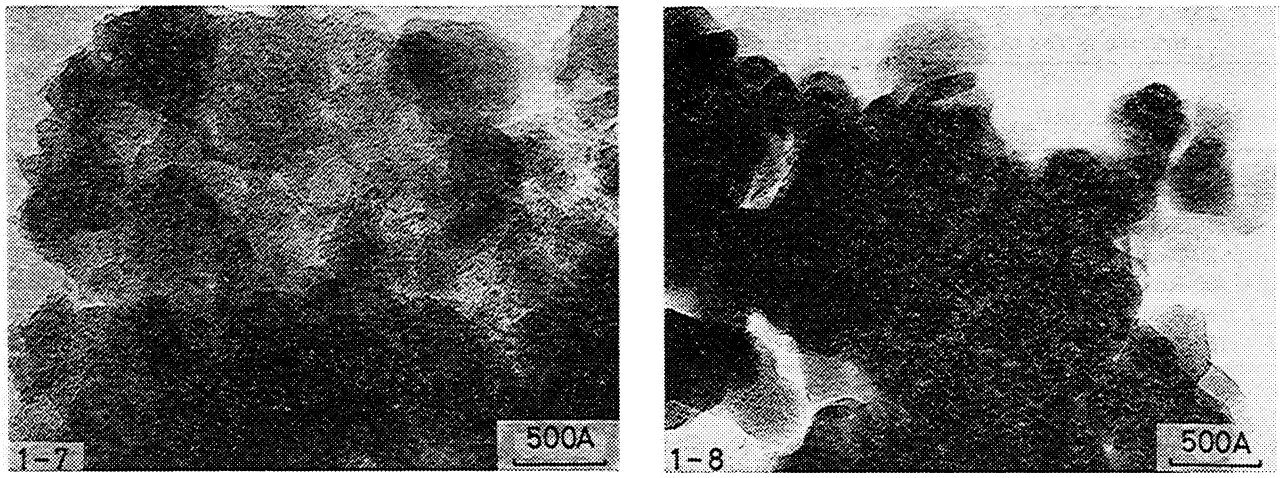

Photo. 1. Transmission electron micrographs of resins heat-treated at 400 °C. (1-1): 2-Resin, (1-2): 2-Resin irradiated with electron beam, (1-3): 10-Resin, (1-4): 10-Resin, (1-5): 30-Resin, (1-6): 40-Resin, (1-7): 100-Resin, (1-8): Furan resin.

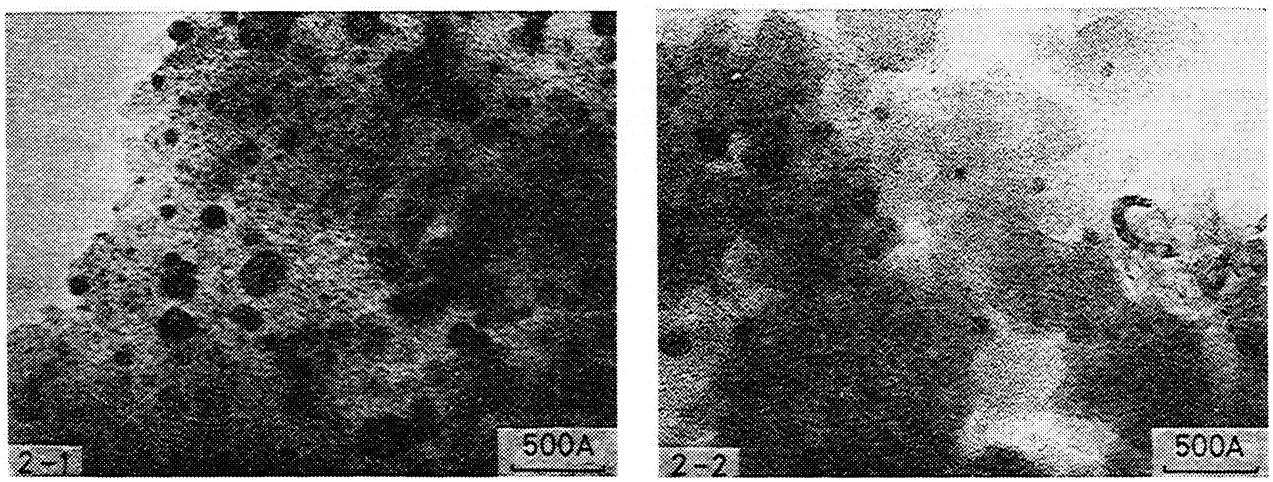

Photo. 2. Transmission electron micrographs of resins heat-treated at 800 °C. (2-1): 2-Resin, (2-2): 100-Resin.

particles in resins (400 °C) did not coagulate to large particles, and their diameters were less than about 200 Å, as is shown in Table 3. Transmission electron micrographs of 2-Resin (800 °C) and 100-Resin (800 °C) are shown in Photo. 2 (2-1, 2-2). The iron particles which were not detected in 100-Resin (400 °C) were observed in 100-Resin (800 °C) as particles 30—200 Å in diameter. The uniformly dispersed iron particles (10—25 Å) coagulated to larger ones with a diameter of more than about 30 Å in 2- to 10-Resins (800 °C). The iron particles of the resins became larger in size than those of the resins, as is shown in Table 3. The pyrophoric phenomenon was due to the presence of the ultra-fine particles less than 200 Å in diameter. The reason for the pyrophoric phenomenon of 10-Resin was explained by the density being lower than those of 2- and 5-Resins and the iron content being higher than those of 20- to 100-Resins. The number of iron particles observed in 30- to 100-Resins (800 °C) was small, but was greater than that of iron particles (30—200 Å) in 2- to 30-Resins (400 °C). The size of the iron particles increased with an increase in the heat-treatment temperature from 1200 to 1500 °C, as is shown in Table 3. The largest iron particles, with a diameter of about 1000 Å, were observed in 10- and 30-Resins (1500 °C). In another resin (1500 °C), the iron particles were not able to coagulate to such large particles. The smallest particles of 2- to 5-Resins (1200 and 1500 °C) were less than those of other resins (1200 and 1500 °C), despite their high iron contents. These results show that the iron particles are finely subdivided in a glasslike carbon matrix, even at high temperatures. The dense glasslike carbon prepared from 2- to 5-Resins was

Table 3. Size of iron particles in heat-treated resins (Å)

Sample	Heat treatment (°C)			
	400	800	1200	1500
2-Resin	10—150	30—200	50—250	50—600
5-Resin	10—200	30—400	50—400	50—500
10-Resin	10—150	30—500	100—600	100—1000
30-Resin	10—100	30—100	100—600	100—1000
40-Resin	<10	30—100	100—500	100—500
100-Resin	<10	30—200	100—200	100—500

Table 4. X-Ray analysis of iron particles dispersed in the glasslike carbon matrix

Sample	Heat treatment (°C)			
	400	800	1200	1500
2-Resin	$\alpha'+\varepsilon$	α	α	α
5-Resin	$\alpha'+\varepsilon$	α	α	α
10-Resin	$\alpha'+\varepsilon$	α	α	α
20-Resin	—	α	α	α
30-Resin	—	—	α	α
40-Resin	—	—	α	α
100-Resin	—	—	α	α

α': expanded bcc Fe, $a_0=2.95$. α: bcc Fe, $a_0=2.86$—2.87. ε: hcp Fe, $a_0=3.30$, $c_0=5.21$.

excellent in its dispersion of iron particles. The observed iron particles were nearly spherical. No characteristic shape related to the crystal structure was found.

Structural Analysis. The crystal structure of iron particles dispersed in the glasslike carbon matrix was analyzed using the X-ray diffraction data. The results are summarized in Table 4. In the X-ray diffraction patterns of 2- to 10-Resins (400 °C), lines based on two kinds of crystals were observed. One of the crystals consisted of expanded, body-centered cubic (bcc) iron, and its unit cell was $a_0=2.95$, larger than that of standard bcc iron (Ref. 29, $a_0=2.8664$). The other crystal consisted of hexagonal, close-packed (hcp) iron. The hcp iron is a high-pressure phase.[30] In the X-ray diffraction of the high-pressure-phase iron, the six diffraction lines are interpreted as being 101, 100, 110, 112, 002, and 103.[31] As is shown in Table 5, these lines

Table 5. X-ray diffraction data of the ultra-fine iron particle in 2- to 10-resins (400 °C)

d(Å)	(hkl)
2.85	(100)
2.61	(002)
2.51	(101)
1.61	(110)
1.48	(103)
1.39	(112)
1.30	(004)
1.10	(203)

were also observed in the X-ray diffraction pattern of ultra-fine iron. Moreover, two extra lines in it corresponded to the 004 and 203 lines. In the diffraction pattern of the 2- to 10-Resins (400 °C), the 110 line of hcp iron overlapped with the 200 line of the expanded bcc iron. The size of the unit cell of the high-pressure phase varies with the pressure: $a=2.465$, $c=4.050$, $c/a=1.643$ at 150 kbars; $a=2.421$, $c=3.828$, $c/a=1.580$ at 400 kbars.[31] At an atmospheric pressure of 1, the hcp phase of the binary Fe–C alloy has been prepared by means of a splat quenching; $a_0=2.502$, $c/a=1.643$.[32] The unit-cell size of ultra-fine hcp iron was $a_0=3.30$ and $c_0=5.21$ ($c/a=1.58$). The unit cell of ultra-fine iron was larger than those of the high-pressure phase and the binary alloy. However, the c/a ratio was similar to those of these hcp phases. For 20- to 100-Resins (400 °C), no diffraction lines were observed except for a broad line in the vicinity of $2\theta=50°$. The broad line was thought to be due to the glasslike carbon, since the same line was observed in Furan resin (400 °C). The few iron particles (10—150 Å) that were observed in 20- to 30-Resins (400 °C) did not contribute to the X-ray diffraction line. The line due to the bcc phase was observed in 2- to 20-Resins (800 °C). Its unit-cell size was $a_0=2.86$—2.87, equal to that of the standard bcc iron. While the iron particle was observed in 30- to 100-Resins (800 °C), the diffraction line of the iron particles was not obtained. The iron particles did not coagulate enough to give an X-ray diffraction pattern in these resins. The broad line due to the glasslike carbon was, however, present in these resins (800 °C). X-ray diffraction confirmed the presence of standard bcc iron in 2- to 100-Resins (1200° and 1500 °C), although the iron content of 100-Resin (1500 °C) was lower than 1%. In these resins the iron particles coagulated to become a large iron particle which was adequate for the X-ray diffraction. In 2- to 10-Resins (400 °C), the number of iron particles (30—200 Å) was less than that of 30- to 100-Resins (800 °C). It is most likely that the iron particles (30—200 Å) in 2- to 10-Resins (400 °C) do not reveal any diffraction lines. Therefore, the hcp and expanded bcc irons are interpreted as being iron particles with diameters 10—25 Å. According to the similarity in crystal structure, it is reasonable to imagine that the iron particles grow in this order; the hcp iron, the expanded bcc iron, and the standard bcc iron.

Table 6. Electron-diffraction analysis of iron particles dispersed in heat-treated resins

Sample	Heat treatment (°C)			
	400	800	1200	1500
2-Resin	R+S	R+S	R+S	R+S
5-Resin	R+S	R+S	R+S	R+S
10-Resin	—	R+S	R+S	R+S
20-Resin	—	R+S	R+S	R+S
30-Resin	—	R+S	R+S	R+S
40-Resin	—	R+S	R+S	R+S
100-Resin	—	R+S	R+S	R+S

R: diffraction ring. S: diffraction spot.

The results of the electron-diffraction analysis are shown in Table 6. In the electron-diffraction profiles of 2- and 5-Resins (400 °C), diffraction rings of both hcp iron and expanded bcc iron were observed. Both rings consisted of diffraction spots. The precise dimensions of the unit cell could not be calculated from the diffraction ring. The appearance of spots suggested that the hcp and expanded bcc irons were a single crystal or a polycrystalline. Since their crystal size was less than 25 Å, it was concluded that the polycrystalline could not be formed. In 10- to 100-Resins (400 °C), there existed only a broad ring instead of the diffraction ring

based on the hcp and expanded bcc irons. The broad ring was due to the glasslike carbon. In 30- to 100-Resins (800 °C), the crystal structure of ultra-fine iron particles which were not clarified by the X-ray diffraction analysis was identified as that of the standard bcc iron. The diffraction rings and spots due to the standard bcc iron were observed in all resins (800 to 1500 °C), as is shown in Table 6.

These results lead to the following conclusions. The ultra-fine iron particles are prepared by the heat treatment of acetylferrocene-furfural resin *in vacuo*. The hcp and expanded bcc irons are identified in the ultra-fine iron particles prepared at 400 °C. The unit cell of hcp iron was larger than that of iron metal under a high pressure. Upon heating, both hcp and expanded bcc iron particles coagulate to larger particles to form the standard bcc iron.

The authors would like to thank Mr. Tsutomu Shoji and Mrs. Hide Arai, Tohoku University, for their cooperation in the iron and CH analyses. Thanks are also due to Messrs. Haruo Yotsumoto and Eiichi Watanabe of the Japan Electron Optics Laboratory for their assistance in the electron-microscopic observation.

References

1) K. Kimoto, I. Nishida, and R. Uyeda, *J. Phys. Soc. Jpn.*, **20**, 1963 (1965).
2) K. Kimoto and I. Nishida, *J. Phys. Soc. Jpn.*, **22**, 744 (1967).
3) C. R. Bamford, *Phys. Chem. Glasses*, **3**, 54 (1962).
4) M. O'Horo and R. Steinitz, *Mater. Res. Bull.*, **3**, 117 (1968).
5) L. N. Mulay, D. W. Collins, and W. Fisher, Jr., *Jpn. J. Appl. Phys.*, **6**, 1342 (1967).
6) D. W. Collins and L. N. Mulay, *J. Am. Ceram. Soc.*, **53**, 74 (1970).
7) R. W. J. Wedd, B. V. Liengme, J. C. Scott, and J. R. Sams, *Solid State Commun.*, **7**, 1091 (1969).
8) W. Henning and E. Vogt, *J. Phys. Rad.*, **20**, 277 (1959).
9) F. E. Luborsky and P. E. Lawrence, *J. Appl. Phys.*, **32**, 231S (1961).
10) L. Weil and L. Gruner, *C. R. Acad. Sci.*, **243**, 1629 (1956).
11) J. J. Becker, *Trans. Am. Inst. Metal. Eng.*, **209**, 59 (1957).
12) D. Schultze, *Naturwissenschaften*, **6**, 128 (1960).
13) C. R. Abeledo and P. W. Selwood, *J. Appl. Phys.*, **32**, 229S (1961).
14) A. E. Berkowitz and W. J. Schuele, *J. Appl. Phys.*, **30**, 134S (1959).
15) W. J. Schuele and V. D. Deetscreek, *J. Appl. Phys.*, **32**, 235S (1961).
16) T. K. McNab, H. Micklitz, and P. H. Barrett, *Phys. Rev. B*, **4**, 3787 (1971).
17) H. Micklitz and P. H. Barrett, *Phys. Rev. B*, **5**, 1704 (1972).
18) H. Micklitz and P. H. Barrett, *Phys. Rev. Lett.*, **28**, 1547 (1972).
19) S. Yajima and M. Omori, *Chem. Lett.*, **1972**, 843.
20) S. Yajima and M. Omori, *Chem. Lett.*, **1974**, 277.
21) S. Yajima and M. Omori, *Nature*, **267**, 823 (1977).
22) M. Omori, K. Nagashima, and S. Yajima, *Bull. Chem. Soc. Jpn.*, **50**, 1157 (1977).
23) M. Omori, M. Kurono, and S. Yajima, *Bull. Chem. Soc. Jpn.*, **48**, 1291 (1975).
24) B. Ya, Andreev, L. M. Dyagileva, and G. I. Feklisov, *Dokl. Akad. Nauk SSSR*, **158**, 1348 (1964).
25) M. J. Tricker, E. L. Evans, P. Cadman, N. C. Davies, and B. Bach, *Carbon*, **12**, 499 (1974).
26) A. M. Aksay, "Vacuum Metallurgy," ed by R. F. Bunshah, Reinhold Publishing Co., New York (1958).
27) H. Honda, Y. Sanada, T. Furuta, and H. Teranishi, *Tanso*, No. 46, 2 (1966).
28) D. R. Stull, *Ind. Eng. Chem.*, **39**, 517 (1947).
29) ASTM Powder Diffraction File, No. 6-0696.
30) E. P. Bundy, *J. Appl. Phys.*, **36**, 616 (1965).
31) R. L. Clendenen and H. G. Drickamer, *J. Phys. Chem. Solids*, **25**, 865 (1964).
32) R. C. Ruhl and M. Cohen, *Trans. Met. Soc. AIME*, **245**, 241 (1969).